Available online at www.sciencedirect.com

ScienceDirect

Procedia Engineering 109 (2015) 3 – 7

Procedia Engineering

www.elsevier.com/locate/procedia

XXIII Italian Group of Fracture Meeting, IGFXXIII

Fragmentation of corrosion protection coatings: a combined finite-element discrete-element study

Gabriella Bolzon*, Ruohan Zhang

Department of Civil and Environmental Engineering, Politecnico di Milano, piazza Leonardo da Vinci 32, 20133 Milano, Italy

Abstract

Iron carbonate scales form compact corrosion protection layers on the internal surfaces of pipelines transporting hydrocarbons. Scales can be removed by the action of the fluid flow and by other mechanisms with the consequent development of severe localized damages. A key safety role is therefore played by the adhesion to the metal substrate, which may be identified through indentation tests supplemented by simulation models of the experiment. Eventually, indentation induces the fragmentation of the coating, a phenomenon rather difficult to be reproduced. Some computational issues relevant to the use, in this context, of finite element and discrete element techniques are discussed in this contribution.

Peer-review under responsibility of the Gruppo Italiano Frattura (IGF)

Keywords: protection coatings; indentaion tests; numerical simulation; finite elements; discrete elements.

1. Introduction

Chemical reactions between carbon steel, water and chemical species produce scales that precipitate on the internal surface of pipelines transporting hydrocarbons and form a compact protective layer, which acts as a diffusion barrier and prevents the progress of corrosion [1–4].

An adequate protection against this degradation phenomenon depends on the mechanical properties of the scales and on their adhesion to the steel substrate. These characteristics can be identified from the results of indentation tests since the morphology and the small thickness of these coatings prevent the use of more direct material characterization techniques [5–8].

* Corresponding author. Tel.: +39 02 2300 4319; fax: +39 02 2399 4300.
E-mail address: gabriella.bolzon@polimi.it

Peer-review under responsibility of the Gruppo Italiano Frattura (IGF)
doi:10.1016/j.proeng.2015.06.201

The interpretation of the data collected from indentation is usually supported by a simulation model of the experiment, mostly resting on the finite element (FE) method [8,9]. This approach returns reliable results for metal components as the material response is dominated by large plastic strains [10,11].

In the FE context, separation across interfaces can be simulated by means of cohesive elements [12,13]. On the contrary, extensive damage leading to discontinuous processes like the creation of fracture networks and fragmentation are rather difficult to be reproduced. This limitation fostered the development of discrete element techniques, which consider large assemblies of usually rigid and simply interacting particles, with contact patterns that change continuously as the overall system deforms. This methodology is often applied to granular materials and rock mechanics [14–16].

In the combined finite-element discrete-element approach [17,18], rigid particles are replaced by deformable bodies that can be meshed into finite elements. Mutual interaction is initially defined through cohesive models, as in FE methods, while contact algorithms typical of the discrete framework permit to control the transition to the discontinuous material response in a number of different application fields, ranging from rock blasting to powder technology.

The capabilities of this simulation tool have been tested on the damaging processes induced by indentation on the layer of corrosion products forming on the internal surface of oil pipelines. The main results are discussed in this contribution.

2. The simulation problem

Layers of iron carbonate scales (15–30 μm thick) were grown in a controlled autoclave environment on pipeline steel. The samples were subjected to indentation tests and inspected by scanning electron microscopy [4]. The deformation of these material systems under both sphero-conical (Rockwell [19]) and pyramidal (Vickers [20]) tips induced the separation of the coating from the metal substrate, the removal of the scales in the region around the residual imprint and, in some situation, the formation of cracks in the underneath material.

The observed phenomena could be reproduced only partially by non-linear FE analyses exploiting the features of a commonly available commercial code, including large displacements and large plastic strains [21]. In these simulations, the steel substrate was attributed an elastic-plastic response resting on Hencky-Huber-Mises criterion with isotropic exponential hardening rule, calibrated on the basis of independent results concerning plain metal samples [10,11]. The brittle layer of corrosion products was described by Drucker-Prager plasticity coupled to a phenomenological description of the progressive degradation of the material strength and stiffness. The damage evolution law was specified in terms of fracture energy, with linear dissipation. The material parameters relevant to the coating, reported in Table 1, were defined on the basis of information available from the literature [1–3].

The influence of the internal friction angle and of the fracture energy was evaluated by means of an axis-symmetric model of the Rockwell indentation test. Perfect adhesion between the bulk material and the thin corrosion layer was considered, with either smooth or rough interface between the coating and its substrate as suggested by the micrograph details reported in [4]. The load was applied in a quasi-static manner, through a rigid idealization of the indenter tip.

In this continuum FE approach, damage localizes in the piling up region where scale removal is observed in the experiments, while the material is compacted under the indented tip. A clear shearing mechanism shows up in the case of a smooth separation surface between the coating and its substrate, while the pattern is slightly scattered by the interface roughness. Results closer to the experimental force-penetration curves are obtained for small internal friction angles while the fracture energy value does not influence the output in a significant manner. However, the analyses arrest at the onset of material separation even introducing a cohesive interface in the FE model.

Table 1. Material parameters in the continuum (FE) model.

Component	Young's modulus [GPa]	Poisson ratio	Compression yield limit [MPa]	Internal friction angle	Hardening exponent	Hardening modulus [MPa]	Failure strain	Fracture energy [N/m]
Coating	150	0.3	400	0°–25°	-	60	0.01	700–1300
Substrate	180	0.3	400	0	0.08	-	-	-

Table 2. Mass density and interface parameters in the combined finite-element discrete-element approach.

Component	Density [kg/m^3]	Tensile strength [MPa]	Shear strength [MPa]	Fracture energy [N/m]	Fracture penalty [MPa]	Contact penalty [MPa]
Coating	5240	400	200	2000	1.5×10^2–1.5×10^5	10^3–10^5
Substrate	7800	500	200	4000	1.5×10^2–1.5×10^5	10^3–10^5

The discretized domain visualized in Fig. 1 was implemented in the combined finite-element discrete-element research code Y developed by Munjiza [18]. In this case, the bulk response of either the coating and the substrate was assumed linear elastic while all irreversible phenomena were attributed to the cohesive interfaces placed among the elements, characterized by the bilinear response sketched in Fig. 1 and defined by the quantities:

$$\delta_t = \frac{2h\sigma_t}{p_f}, \quad \delta_u - \delta_t = \frac{2G_f}{\sigma_t}, \quad h = \sqrt{\frac{4A}{\pi}} \tag{1}$$

In the above relationships: δ_t and δ_u indicate the relative displacement in correspondence of the maximum stress transferred by the interface and at complete element detaching, with the constraint $\delta_u \geq 2\delta_t$ imposed by Y code; σ_t represents the material strength in either normal or tangential direction; G_f and p_f constitute the fracture energy and the fracture penalty, respectively; A and h stand for the element area and characteristic size.

The considered parameter values are reported in Table 2. Notice that higher interfacial strength and toughness were attributed to the ductile metal substrate.

A contact penalty coefficient prevents the interpenetration among elements in contact.

Displacements were fully constrained on the bottom side of the investigated region, 1200 μm × 500 μm wide. The critically damped dynamic response of the considered material system under uniformly distributed load was analyzed in plane stress conditions. Therefore, a quantitative comparison with either the FE or the experimental output is not meaningful. However, the main damaging phenomena observed during the tests were reproduced by the combined finite-element discrete-element approach.

Fig. 2 and Fig. 3 show the detaching of the coating layer, mostly sliding over the metal substrate, and some opening displacement developing in the piling up region around the indenter imprint. These phenomena are amplified and scales are removed as the analysis proceeds, while no local unloading is observed anywhere. The formation of a second material separation surface in the coating thickness evidences significant shear gradients.

In these numerical analyses, the irreversible metal deformation due to the development of large plastic strains was replaced by fictitious relative displacements at the interfaces among the discretization elements. The compliance of the substrate under the indenter tip, controlled by the fracture penalty, played an essential role on the coating failure mode, see Fig. 4, although no significant influence on the results was observed in the penalty range 1.5×10^2 to 1.5×10^3.

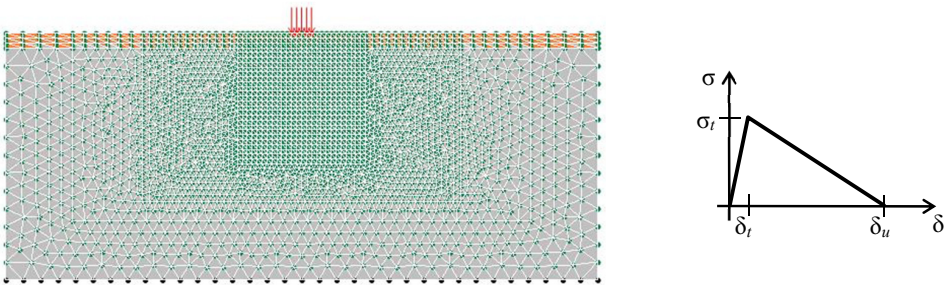

Fig. 1. Simulation and interface model in the analyses performed by the combined finite-element discrete-element research code Y [18].

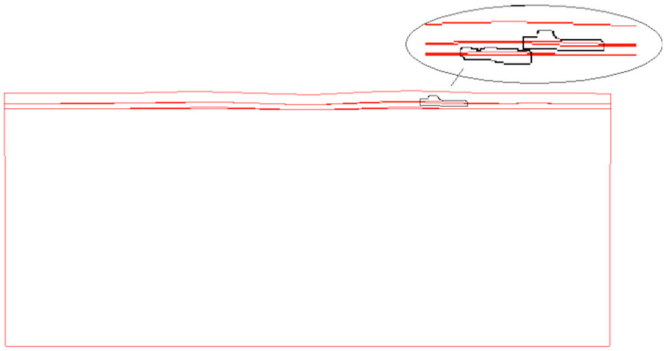

Fig. 2. Initial material separation pattern (0.025 ms time, fracture penalty 1.5×10^2).

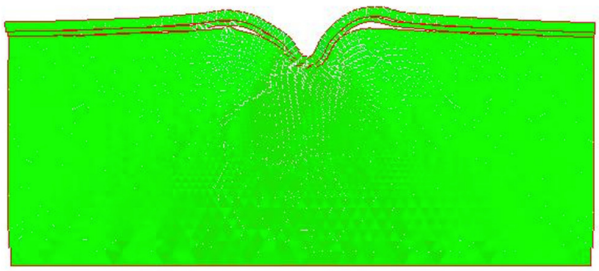

Fig. 3. Fragmentation of the corrosion layer (2.5 ms time; fracture penalty 1.5×10^2).

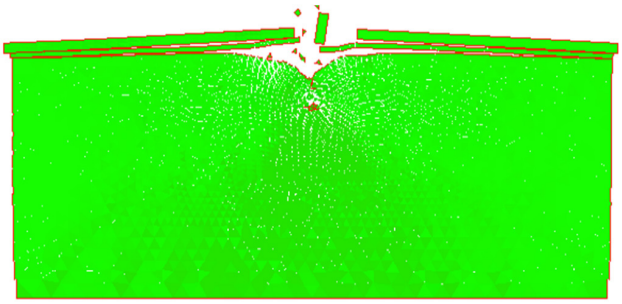

Fig. 4. Failure pattern for fracture penalty 1.5×10^5 (2.5 ms time).

3. Closing remarks

The capabilities of a computational approach based on combined finite-element discrete-element techniques have been tested on the simulation problem of the damaging phenomena induced by indentation on the layer of corrosion products forming on samples of oil pipeline steel.

A preliminary investigation was performed on a rough idealization of the real material system implemented in the research code Y, developed by Munjiza [18]. Despite the several limitations of the considered model, the main observed features of the experimental response were reproduced, including the removal of scales in correspondence of the piling up region around the imprint left by the indenter tip on the sample surface.

A quantitative comparison would require to replace the plane stress conditions with an axis-symmetric simulation, or to perform a more demanding three-dimensional analysis. The interplay among the model parameters, which govern the response of the investigated material system should be evidenced.

The fictitious representation of the large plastic deformation developing on the substrate by relative displacements at the interface among the discrete elements should be also validated. In the present context, however, the focus of the analysis is on the corrosion layer and on the adhesion with the underneath material while the discretization of the metal region plays the major role of inducing realistic boundary conditions at the interface between the coating and its support.

References

[1] C.A. Palacios, J.R. Shadley, Characteristics of corrosion scales on steels in a CO_2-saturated NaCl brine, Corrosion 47 (1991) 122–127.
[2] K. Gao, F.Yu, X. Pang, G. Zhang, L. Qiao, W. Chu, M. Lu, The relationship between fracture toughness of CO_2 corrosion scale and corrosion rate of X65 pipeline steel under supercritical CO_2 condition, Corrosion Sci. 50 (2008) 2796–2803.
[3] Y. Zhang, X. Pang, S. Qu, X. Li, K. Gao, Mechanical properties of CO_2 corrosion product scales and their relationship to corrosion rates, Int. J. Greenhouse Gas Control 5 (2011) 1643–1650.
[4] G. Bolzon, G. Gabetta, B. Molinas, An investigation on corrosion protection layers in pipelines transporting hydrocarbons, Fratt. Integr. Strutt. 30 (2014) 31–39.
[5] ISO 14577–1, Metallic materials – Instrumented indentation test for hardness and materials parameters – Part 1: Test method, Geneva, 2002.
[6] ISO/TR 29381, Metallic materials – measurement of mechanical properties by an instrumented indentation test – Indentation tensile properties, Geneva, 2008.
[7] B. Bhushan, X. Li, Nanomechanical characterisation of solid surfaces and thin films, Int. Mater. Rev. 48 (2003) 125–164.
[8] G. Bolzon, M. Bocciarelli, E.J. Chiarullo, Mechanical characterization of materials by micro-indentation and AFM scanning, in: Applied scanning probe methods XII – Characterization, B. Bhushan and H. Fuchs (Eds.), Springer, Berlin (2008) 85–120.
[9] G. Bolzon, G. Maier, M. Panico, Material model calibration by indentation, imprint mapping and inverse analysis, Int. J. Solids Struct. 41 (2004) 2957–2975.
[10] G. Bolzon, B. Molinas, M. Talassi, Mechanical characterisation of metals by indentation tests: an experimental verification study for on-site applications, Strain 48 (2013) 517–527.
[11] G. Bolzon, G. Gabetta, B. Molinas, Integrity assessment of pipeline systems by an enhanced indentation technique, ASCE J. Pipeline Sys. Eng. Pract. 6 (2015) 04014010.
[12] G. Bolzon, M. Bocciarelli, Indentation and imprint mapping for the identification of constitutive parameters of thin layers on substrate: Perfectly bonded interfaces, Mat. Sci. Eng. A, 448 (2007) 303–314.
[13] M. Bocciarelli, G. Bolzon, Indentation and imprint mapping for the identification of interface properties in film-substrate systems, Int. J. Fracture, 155 (2009) 1–17.
[14] P.A. Cundall, A computer model for simulating progressive, large scale movements in blocky rock systems, Int. Symp. on Rock Mechanics, Vol. I, Int. Soc. Rock Mech., Nancy, France, 1971.
[15] L. Jing, A review of techniques, advances and outstanding issues in numerical modelling for rock mechanics and rock engineering, Int. J. Rock Mech. Min. Sci. 40 (2003) 283–353.
[16] D.O. Potyondy, P.A. Cundall, A bonded-particle model for rock, Int. J. Rock Mech. Min. Sci. 41 (2004) 1329–1364
[17] A. Munjiza, D.R.J. Owen, N. Bicanic, A combined finite-discrete element method in transient dynamics of fracturing solids. Int. J. Eng. Computations, 12 (1995) 145–174.
[18] A.Munjiza, The Combined Finite-Discrete Element Method, Wiley, Chichester, 2004.
[19] ISO 6508–1, Metallic materials – Rockwell hardness test – Part 1: Test method (scales A, B, C, D, E, F, G, H, K, N, T), International Organization for Standardization, Geneva, 2005.
[20] ISO 6507–1, Metallic materials – Vickers hardness test – Part 1: Test method, International Organization for Standardization, Geneva, 2005.
[21] G. Bolzon, A. Cornaggia, G. Gabetta, Fracture of corrosion protecting layers: investigation by indentation test, 19th European Conference on Fracture (ECF19), Kazan, Russia, 2012.